

Observational Study

Anatomic Evaluation of the Sacroiliac Joint: A Radiographic Study with Implications for Procedures

Sumit H. Rana, MD¹, Payam Farjoodi, MD¹, Sean Haloman, MD¹, Pascual Dutton, MD¹,
Arvin Hariri, MD², Samuel R. Ward, PT, PhD^{1,2}, Steven R. Garfin, MD¹,
and Douglas G. Chang MD, PhD¹

From: Departments of
¹Orthopaedic Surgery and
²Radiology, University of
California San Diego, USA

Address Correspondence:
Douglas Chang, MD, PhD.
Department of Orthopaedic
Surgery
University of California,
San Diego
200 West Arbor Drive,
Suite 121
San Diego, CA 92103-8894
E-mail:
dchang@ucsd.edu

Disclaimer: There was
no external funding in
the preparation of this
manuscript.

Conflict of interest: Dr
Garfin reports a financial
interest in SI Bone, Inc.,
outside the submitted work.

Otherwise the authors
report no conflicts of
interest.

Manuscript received:
09-10-2014

Revised manuscript
received:
05-21-2015

Accepted for publication:
06-17-2015

Free full manuscript:
www.painphysicianjournal.
com

Background: Sacroiliac joint (SI) pain is increasingly being recognized as a source of low back pain. Injections and percutaneous type procedures are performed to treat symptomatic joints. However, there are limited studies available assessing the anatomy of the SI joint in vivo among patients with pain.

Objectives: The purpose of this study was to provide more precise information on the dimensions and orientation of the SI joint using a new technique for the radiographic evaluation of this joint.

Study Design: Observational study.

Setting: Emergency department

Methods: Three dimensional computed tomographic (CT) reconstructions of the pelvis were formatted from 100 SI joints in 50 patients who had clinically indicated abdominal/pelvic scans. These images were manipulated to evaluate the SI joint in multiple planes and measure its dimensions, area, and relationship to anatomic landmarks such as the anterior superior iliac spine (ASIS) and posterior superior iliac spine (PSIS).

Results: Of the 50 patients, 23 were men and 27 women. Their mean age was 47.6 years (\pm 18.1). The SI joint consists of a superior limb which measures 39.7 mm (\pm 4.8) in length, and an inferior limb which measures 54.3 mm (\pm 5.1), oriented at an angle of 100.1° (\pm 8.1) to one another. The mean area of the joint was 1276.8 mm² (\pm 189.8). The horizontal distance from the ASIS to the front of the superior SI joint is 75.4 mm (\pm 8.4). The horizontal distance from the PSIS to the back of the superior SI joint is 43.9 mm (\pm 5.6). The joint stretches 7.5 mm (\pm 5.9) cephalad and 38.1 mm (\pm 6.4) caudal to the PSIS, and 35.4 mm (\pm 8.8) cephalad and 10.2 mm (\pm 11.4) caudal to the ASIS.

Limitations: CT scans were performed with patients lying supine, while most SI joint procedures are performed with a patient prone. However it is doubtful that the bony anatomic landmarks would change appreciable in this largely immobile joint. These patients were seen in the emergency department for a variety of conditions related to abdominal and pelvic pain, and not exclusively for SI joint pain.

Conclusions: Treatment of the SI joint by surgeons and interventionalists is hampered by the limited number of anatomic studies in the literature. Our study presents the SI joint as a 2-limbed structure, sitting from slightly above the level of the PSIS rostrally to slightly below the level of the ASIS caudally. Palpation of these landmarks may assist in directing physicians to the joint. To begin an interventional pain procedure, with a patient lying prone, this data supports tilting the x-ray image intensifier 10 degrees caudal past the vertical anteroposterior (AP) view for optimal approach of the SI joint's inferior limb. The needle entry should be about 44.1 mm (1.75 inches) caudal to the PSIS. The image intensifier should have a 12 degree left lateral oblique view for injection of the right SI joint, and a 12 degree right lateral oblique view for the left SI joint.

Key words: Sacroiliac joint, arthriti, sacroiliac, anatomy, injections, intra-articular, tomography, x-ray computed, imaging, three-dimensional, pain management, back pain, radiology

Pain Physician 2015; 18:583-592

Sacroiliac (SI) joint pain is increasingly being recognized as a potential primary source of low back pain. The prevalence of the SI joint being the source of low back pain appears to be in the 15 – 25% range (1-4). Treatments of SI joint pain involve non-operative and operative options. Non-operative treatment options include medications, physical therapy, orthotics, and manual manipulation. Interventional treatment includes injections, viscosupplementation, radiofrequency neurotomy, and arthrodesis, with new minimally invasive fusion techniques now available.

Surgical procedures are used to “stabilize” the SI joint to help decrease pain presumed to originate there due to degenerative disease, instability, dysfunction, and post-traumatic arthritis, among other conditions. Additionally, SI injections and other percutaneous procedures are available for diagnosis and pain relief. However, there are few studies in the literature which describe the three-dimensional (3-D) anatomy of the SI joint. A clearer understanding of the anatomy will help physicians treat the SI joint. Knowing the relationship of the SI joint relative to the anterior superior iliac spine (ASIS), and posterior superior iliac spine (PSIS) can help physicians localize the SI joint for injections as well as for surgery, and may decrease the radiation associated with procedures directed to the joint.

The SI joint is the largest axial joint in the human body, with an average surface area of 17.5 cm² (5). It has been described as auricular in shape, and is classified as a diarthrodial synovial joint (6). Interestingly, even though it is classified as a synovial joint, 75% of its superior joint surface is not synovial (7). The joint capsule is divided into an anterior and posterior portion. The anterior portion is comprised of a thin capsule and overlying ligament which blend into the iliolumbar ligament. The posterior capsule is often rudimentary or absent. The dorsal SI ligaments are thick and robust, and function as a connecting band between the sacrum and ilia (8). In addition to these ligaments, the joint is supported by a network of muscles including the gluteus maximus and medius, erector spinae, latissimus dorsi, biceps femoris, psoas, piriformis, and oblique and transversus abdominis muscles, as well as by the thoracodorsal fascia. To make things more complicated, the SI joint also varies widely between individuals, as well as from side to side in the same individual (7). In addition, there are also age-related changes in the SI joint. These changes start at puberty and continue throughout life.

The purpose of this study was to provide more precise information on the dimensions and orientation of

the SI joint, using a new technique for the radiographic evaluation.

METHODS

Fifty consecutive patients with computed tomography reconstructions (CTs) of the abdomen and pelvis performed at our institution were selected. Because this project involved de-identified images, institutional research board approval was not required. The indications for these exams involved clinical conditions of pain, suspected nephrolithiasis, hematuria, cancer, and trauma (listed in order of the indication frequency). The CTs were obtained on one of 3 CT scanners: GE Discovery HD750 64 Slice, Toshiba Aquilion 16, or a GE Lightspeed 4 Slice scanner. Multiple helical images were obtained through the abdomen and pelvis, according to standard protocols. For each patient, contiguous axial CT images of the pelvis were imported into a Toshiba Vitrea workstation using the Vitrea 2 analysis system (versions 3.8 and 4.3, Tustin, CA, USA), into the Vitrea workstation (Vitrea 2, versions 3.8 and 4.3), a software application produced by Toshiba which is utilized for more complex image manipulation and analysis than can typically be performed on a Picture archiving and communications system (PACS) workstation. On the Vitrea workstation, maximum-intensity projection (MIP) 3-D reformatted images of the bony sacro-pelvic complex were obtained. A free-hand region of interest was used to define the pelvic portion of the sacro-pelvic complex, which was then subtracted from the reformatted images, leaving behind only the sacral portion of the SI joint.

Figs. 1 and 2 show how subtraction of the ilium allowed for visualization of the sacral portion of the sacro-iliac joint. Fig. 3 shows the division of the SI joint into 2 limbs: a superior and an inferior limb.

On the Vitrea workstation, horizontal lines were drawn joining the ASISs and separately, the PSISs, which we refer to as the inter-ASIS and inter-PSIS lines, respectively. The Vitrea-generated 3-D reformats allowed for measurement of the following parameters: length of the superior and inferior limbs of the SI joint (see Fig. 4), surface area of the joint (see Fig. 5), horizontal distance from the inter-ASIS line to the anterior aspect of the SI joint, horizontal distance from the inter-PSIS line to the anterior aspect of the SI joint, and the vertical position of the joint relative to the inter-ASIS and inter-PSIS lines, respectively (see Figs. 6 and 7).

For each patient, the Vitrea workstation was used to trace out the superior and inferior limbs of the SI joint (shown in Fig. 3). Then, the software was used to

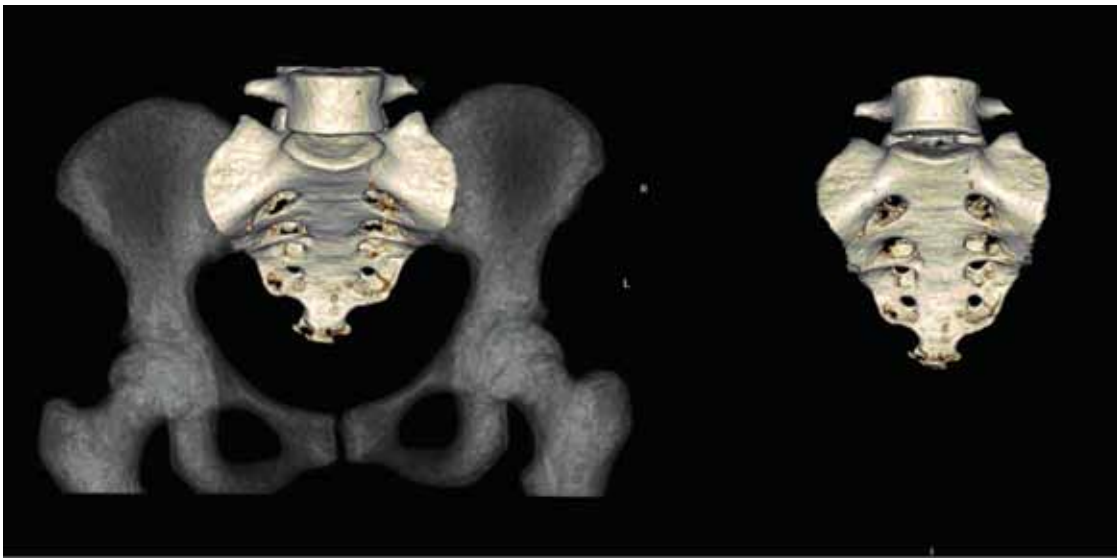


Fig. 1. The Vitrea workstation allowed for virtual subtraction of the bony pelvis, so that the SI joint could be evaluated. The image on the left is a 3-D MIP image of the pelvis in AP projection, while the image on the right is a 3-D MIP image of only the sacrum in AP projection, obtained by user-defined selection and subtraction of the bony pelvis. These images can be rotated and manipulated in any plane; for our study, the sacrum was oriented in the sagittal plane.

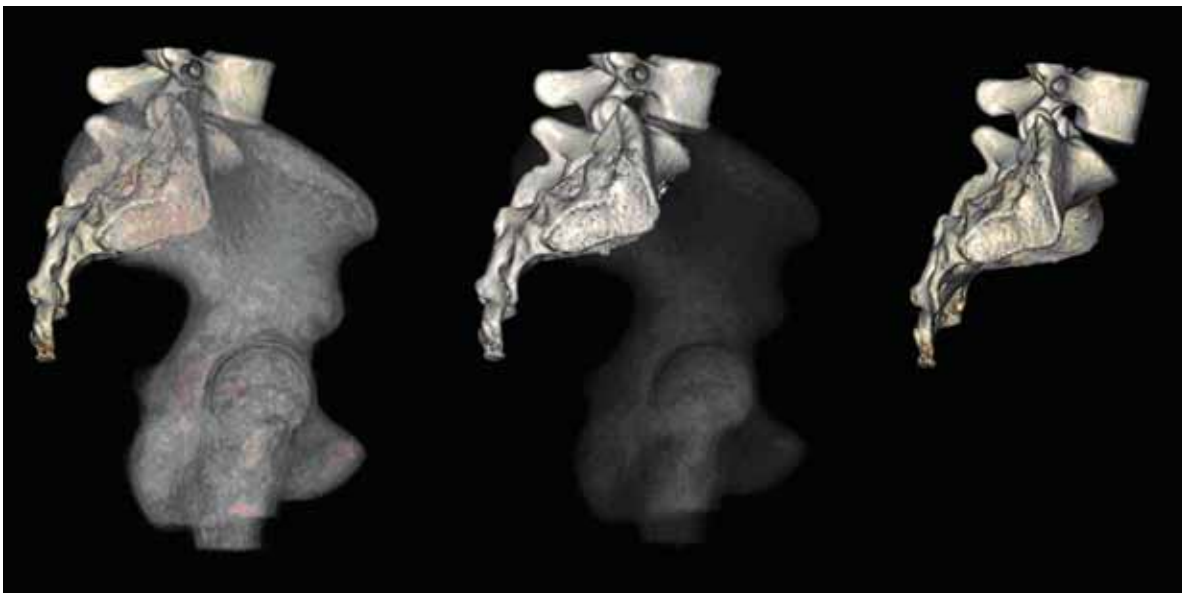


Fig. 2. Images both pre- (far left) and post- (far right) subtraction of the bony pelvis in the sagittal plane, performed on the Vitrea workstation. The middle image is after removal of only the right hemipelvis. Sagittal images allow visualization of the articular surface of the sacrum en face.

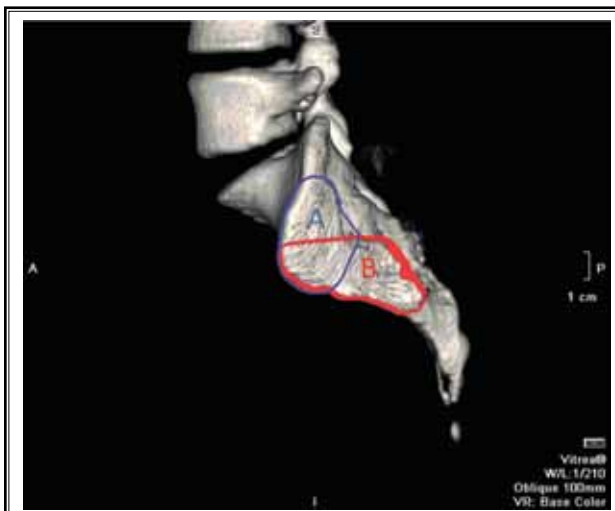


Fig. 3. The SI joint has 2 limbs: the superior limb, A (in blue), and the inferior limb, B (in red).



Fig. 4. The lengths of the superior and inferior limbs of the SI joint (labeled A and B, respectively) were measured along the long axes of these limbs. The angle between the long axes of these limbs was also calculated.



Fig. 5. The surface area of the SI joint was calculated by the Vitrea workstation.

construct the longest line along the long axis of each limb. Due to small variations in how these long axis lines could be constructed, these lines were produced 3 times, and the mean value of those measurements was utilized. The standard deviation of these repeat measurements was on the order of 0.47 mm, about 0.7% of the measurement, and much smaller than the inter-patient variability as reported in Table 1. The inter-limb angles, as shown in Fig. 5, were similarly calculated 3

times. The surface area of the entire joint was outlined, and the Vitrea workstation calculated the surface area of the entire sacral surface of the SI joint. Again, this measurement was performed 3 times, and the average of those measurements was used to represent the average surface area of the SI joint.

In the axial plane, SI joint angulation was measured using the CT images in the following fashion: The caudal part of the SI joint was chosen, a horizontal line was drawn across the posterior border of the sacrum, and then a line was brought down through the right and left SI joints.

To calculate the horizontal distance from the inter-ASIS line to the anterior aspect of the superior limb of the SI joint, the authors identified the ASIS on the anteroposterior (AP) shown in Fig. 6. The inter-ASIS line was then drawn connecting the left and right ASIS. This inter-ASIS line maintained its relative position in 3-D space, while the image was rotated, and the distance from the ASIS to the superior aspect of the joint and to the inferior aspect of the joint could be measured. Through similar manipulation, the horizontal distance from the ASIS to the anterior aspect of the superior limb of the SI joint was measured. The same measurements were performed using the PSIS as a reference point.

There were 50 patients used in this anatomic evaluation; 23 were men and 27 were women. The mean age of the patient population was 47.6 years (range 20 – 85). The mean age of the men was 44.7 years (range 20



Fig. 6. In the AP projection, the ASIS was easily identified. The inter-ASIS line was then constructed, and maintained its relative position in 3-D space during image rotation. In the sagittal plane, the vertical distances between the inter-ASIS line and the most superior and inferior aspects of the SI joint could be measured. Also in the sagittal plane, the horizontal (anteroposterior) distance from the inter-ASIS line to the most anterior aspect of the SI joint was measured.



Fig. 7. In the AP projection, the PSIS was easily identified. The inter-PSIS line was then constructed, and maintained its relative position in 3-D space during image rotation. In the sagittal plane, the vertical distances between the inter-PSIS line and the most superior and inferior aspects of the SI joint could be measured. Also in the sagittal plane, the horizontal (anteroposterior) distance from the inter-PSIS line to the most anterior aspect of the SI joint was measured.

– 83), and the mean age of the women was 49.9 years (22 – 85). There was no statistical difference between the ages in the 2 groups ($P = 0.313$).

Statistical Analysis

After screening the data for normality and homogeneity of variances, we used a multivariate approach to compare genders, sides (R vs L), and the interaction between gender and sides. This approach yielded a statistical evaluation of genders and sides, while cor-

Table 1. Summary of all patients: men ($n = 23$), women ($n = 27$).

Variable	Mean	Standard Deviation	95% Confidence Interval
Length of Superior Limb (in mm)	39.7	4.8	38.4 – 39.5
Length of Inferior Limb (in mm)	54.3	5.1	52.9 – 55.8
Surface area of SI joint (in mm ²)	1276.8	189.8	1222.8 – 1330.7
Horizontal distance from ASIS to SI joint (in mm)	75.4	8.4	73.0 – 77.8
Horizontal distance from PSIS to SI joint (in mm)	43.9	5.6	42.3 – 45.5
Vertical distance from PSIS to top of SI joint (in mm)	7.5	5.9	5.8 – 9.1
Vertical distance from PSIS to bottom of SI joint (in mm)	38.1	6.4	36.3 – 39.9
Vertical distance from ASIS to top of SI joint (in mm)	35.4	8.8	32.9 – 37.9
Vertical distance from ASIS to bottom of SI joint (in mm)	10.2	11.4	6.94 – 13.4

recting for the correlation among dependent variables. Following this overall test, separate 2-way repeated measures ANOVAs (gender x side) were used for each dependent variable, and post-hoc Tukey's tests were used to identify specific differences when main effects were present. SPSS statistical software (Version 20.0, IBM, Armonk, NY) was used for all analyses with a significance threshold of $\alpha = 0.05$. Data are presented as mean \pm standard deviation unless otherwise noted.

RESULTS

The SI joint consists of a superior limb and inferior limb. When looking at all 50 patients as one group, not controlling for gender or side-to-side differences, the mean length of the superior limb was 39.7 mm (± 4.8), and the mean length of the inferior limb was 54.3 mm (± 5.1). The 2 limbs were oriented at a mean angle of 100.1° (± 8.1) to one another. The mean surface area of the joint was calculated to be 1276.8 mm² (± 189.8). Multivariate ANOVA demonstrated a statistically significant difference between men and women ($P < 0.001$). (For summary, see Table 1.)

For men only, the mean length of the superior limb was 41.5 mm (± 5.3), and the mean length of the inferior limb was 57.8 mm (± 3.6). The 2 limbs were oriented at a mean angle of 102.5° (± 5.7) to one another in the sagittal plane. With the patient lying supine, the caudal aspect of the joint was oriented 11.5 degrees (± 4.0) off vertical in the axial plane. The mean surface area of the joint was 1419.1 mm² (± 136.5). The horizontal distance from the ASIS to the front of the superior SI joint was 79.0 mm (± 6.0). The horizontal distance from the PSIS to the dorsal bone edge of the superior SI joint was 46.0 mm (± 4.8). The joint was 6.8 mm (± 6.7) cephalad to and 42.4 mm (± 5.1) caudal to the PSIS, and 31.3 mm (± 9.2) cephalad to and 17.7 mm (± 10.8) caudal to the ASIS. (For summary, see Table 2.)

For women only, the mean length of the superior limb was 38.2 mm (± 4.0), and the mean length of the inferior limb was 51.4 mm (± 4.1). The 2 limbs were oriented at a mean angle of 98.0° (± 6.0) to one another in the sagittal plane. With the patient lying supine, the caudal aspect of the joint was oriented 11.8 degrees (± 6.5) off vertical in the axial plane. The mean surface area of the joint was calculated to be 1155.5 mm² (± 137.6). The horizontal distance from the ASIS to the front of the superior SI joint was 72.5 mm (± 9.1). The horizontal distance from the PSIS to the back of the superior SI joint was 42.2 mm (± 5.7). The joint stretched from 8.0 mm (± 5.0) cephalad to and 34.4 mm (± 4.9) caudal to the PSIS, and 38.9 mm (± 6.8) cephalad to and 3.8 mm (± 7.5) caudal to the ASIS. (For summary, see Table 3.)

There was a statistical difference between men and women in terms of the length of the superior limb of the SI joint ($P = 0.017$), the length of the inferior limb of the SI joint ($P < 0.001$), and the surface area of the SI joint ($P < 0.001$). The SI joint in the men was translated more inferiorly, relative to the ASIS, than in the women. Also there were statistically significant differences in terms of the relationship between the SI joint and the ASIS and PSIS. Table 4 summarizes the difference between the men and women.

Multivariate ANOVA assessment demonstrated a statistically significant difference between the left and right joints ($P < 0.001$). There was a significant difference between the left and right SI joints for the position of the SI joint relative to the ASIS. Using the ASIS as a landmark, the upper edge of the right SI joint was on average 3.1 mm (± 0.96 S.E., $P = 0.003$) lower than the upper edge of the left SI. Similarly, the caudal edge of the right SI joint was on average 2.5 mm (± 1.02 S.E., $P = 0.017$) lower than the caudal edge of the left SI. When the PSIS was used as an anatomic landmark, a similar relationship was seen, but it was not as statisti-

Anatomic Evaluation of the Sacroiliac Joint

Table 2. Summary of male patients.

Variable	Mean	Standard Deviation	95% Confidence Interval
Length of Superior Limb (in mm)	41.5	5.3	39.2 – 43.8
Length of Inferior Limb (in mm)	57.8	3.6	56.3 – 59.4
Surface area of SI joint (in mm ²)	1419.1	136.5	1360.1 – 1478.2
Horizontal distance from ASIS to SI joint (in mm)	79.0	6.0	76.3 – 81.6
Horizontal distance from PSIS to SI joint (in mm)	46.0	4.8	43.9 – 48.1
Vertical distance from PSIS to top of SI joint (in mm)	6.8	6.7	3.92 – 9.71
Vertical distance from PSIS to bottom of SI joint (in mm)	42.4	5.1	40.2 – 44.6
Vertical distance from ASIS to top of SI joint (in mm)	31.3	9.2	27.3 – 35.3
Vertical distance from ASIS to bottom of SI joint (in mm)	17.7	10.8	13.0 – 22.3

Table 3. Summary of female patients.

Variable	Mean	Standard Deviation	95% Confidence Interval
Length of Superior Limb (in mm)	38.2	4.0	36.7 – 39.8
Length of Inferior Limb (in mm)	51.4	4.2	49.7 – 53.0
Surface area of SI joint (in mm ²)	1155.5	137.6	1101.1 – 1210.0
Horizontal distance from ASIS to SI joint (in mm)	72.5	9.1	68.8 – 76.1
Horizontal distance from PSIS to SI joint (in mm)	42.2	5.7	39.9 – 44.4
Vertical distance from PSIS to top of SI joint (in mm)	8.0	5.0	6.0 – 10.1
Vertical distance from PSIS to bottom of SI joint (in mm)	34.4	4.9	32.5 – 36.3
Vertical distance from ASIS to top of SI joint (in mm)	38.9	6.8	36.2 – 41.6
Vertical distance from ASIS to bottom of SI joint (in mm)	3.8	7.5	0.9 – 6.8

Table 4. Comparison of men to women.

Variable	Mean Difference (Men – Women)	P-value
Length of Superior Limb (in mm)	3.2	0.017***
Length of Inferior Limb (in mm)	3.4	< 0.001***
Surface area of SI joint (in mm ²)	263.6	< 0.001***
Horizontal distance from ASIS to SI joint (in mm)	6.5	0.005***
Horizontal distance from PSIS to SI joint (in mm)	3.8	0.014***
Vertical distance from PSIS to top of SI joint (in mm)	-1.2	0.484
Vertical distance from PSIS to bottom of SI joint (in mm)	8.0	< 0.001***
Vertical distance from ASIS to top of SI joint (in mm)	-7.6	0.002***
Vertical distance from ASIS to bottom of SI joint (in mm)	13.8	<0.001***

cally robust as the ASIS data. Because the difference in the length and surface area of the right versus left SI joint was not statistically significant, this implied that the SI joint on the right is translated more inferiorly relative to the ASIS than the left SI joint. Table 5 summarizes the difference between right versus left SI joint measurements.

Overall, the men had a larger SI joint than women

in terms of length and surface area. The SI joint in men was translated more inferiorly relative to the ASIS than in the women. In men and women, the SI joint on the right was translated more inferiorly relative to the ASIS than the left SI joint.

DISCUSSION

Diagnosing SI joint-mediated pain is challenging.

Table 5. Comparison of right versus left.

Variable	Mean Difference (Right – Left)	P-value
Length of Superior Limb (in mm)	0.1	0.921
Length of Inferior Limb (in mm)	-1.3	0.117
Surface area of SI joint (in mm ²)	19.8	0.110
Horizontal distance from ASIS to SI joint (in mm)	-0.9	0.297
Horizontal distance from PSIS to SI joint (in mm)	0.3	0.496
Vertical distance from PSIS to top of SI joint (in mm)	-1.0	0.124
Vertical distance from PSIS to bottom of SI joint (in mm)	0.9	0.116
Vertical distance from ASIS to top of SI joint (in mm)	-3.1	0.003***
Vertical distance from ASIS to bottom of SI joint (in mm)	2.5	0.017***

Pain from the SI joint is usually referred to an area inferior to the PSIS. Such patients rarely have pain above the L5 level (4,7). Because of its anatomic location, the SI joint is difficult to isolate on history and exam as a source of pain because there are many well-recognized pain-sensitive structures nearby, such as the lumbar discs, nerve roots, facet joints, hip joints, muscles, etc. which can refer pain to the SI region (5,9). Imaging modalities including CT and bone scan have been equally disappointing in discerning the SI joint as the source of low back pain. Elgafy et al (10), in a retrospective analysis, reported a 57.5% sensitivity and 69% specificity of CT scan imaging in the diagnosis of the SI joint pain as the source of the patients' pain. Maigne et al (11) and Slipman et al (12) found radionuclide bone scanning to have a sensitivity of 46% and 13%, respectively, and a specificity of 89.5% and 100%, respectively. One intervention that has been demonstrated useful in diagnosing this condition is fluoroscopically guided, or CT-guided, injections of the SI joints (6). Currently these interventions are the most commonly used test to confirm the diagnosis, and there is a good level of evidence to support the use of injections for this diagnostic purpose (13).

However, among interventional pain management physicians, there is recognition that this intervention can be challenging to perform accurately (14,15). Particularly with older, osteoporotic bone, it can be difficult to confirm precise intra-articular placement of the needle and/or contrast. Positive and negative responses to an injection may occur for a variety of reasons, such as extravasation of medication out of a joint with anatomic defects, inability of the medication to reach the painful areas of this complex joint, and incorrect needle placement resulting in vascular, ligamentous, or osseous injection. Zou et al (15) recently conducted a small

clinical study, involving x-ray guided SI joint injections with confirmatory post-injection CT scanning. They described the procedural challenges of the injections, and reported successful confirmation of an intra-articular injection in 13 of 20 (65%) of their patients. All of these factors may explain why there is only "limited" evidence to support the use of SI injections therapeutically (13,16).

In addition to image-guidance, knowing the precise anatomy of the joint and its average distance from easily palpable landmarks, like the ASIS and PSIS, could make these injections easier to perform and improve radiation exposure. For example, the anatomic data presented in this paper suggests a specific fluoroscopic approach for injection of the SI joint. With a patient lying prone, the data supports using a tilt of the x-ray image intensifier 10 degrees caudal past the vertical AP view for optimal approach of the SI joint's inferior limb. The needle entry point should be about 44.1 mm (1.75 inches) caudal to the PSIS. The image intensifier should have a 12-degree left lateral oblique view for the right SI joint and a 12-degree right lateral oblique view for the left SI joint.

In our study, we have elucidated the anatomy of the SI joint and the differences in this anatomy between men and women, and the left and right side. When using the ASIS as a surface anatomy landmark, the entire SI joint was about 3 mm lower on the right than the left SI joint, which is consistent with Dreyfus et al's observations (7). In addition, in general, when comparing men to women, the men's SI joints were translated inferiorly compared to women. The superior edge of a male SI joint was roughly 7 – 8 mm lower than that of a female SI joint, when the ASIS is used as a surface anatomy landmark. The inferior edge of the male SI joint was roughly 13 – 14 mm lower than

the inferior edge of a female SI joint. These results are not surprising as the bony anatomy of the male pelvis is known to be different than the female pelvis.

Zou et al (15) recently published a study of SI joint anatomy. They too observed male-female dimension differences in SI joint anatomy. Furthermore, in an x-ray guided, "practice-based" component of their study, involving 20 patients, they suggested a needle approach angle of 90 degrees due to the "almost parallel" SI joint. Our 3-D data from 50 CT scans, suggests 12 degrees oblique off midline and 10 degrees caudal off vertical is ideal. How our results compare with their CT scan results otherwise is difficult to evaluate. They did not specify the imaging plane used to make their measurements, so it is unclear actually where along the SI joint their data reference. They did not specify the experimental uncertainty and repeatability of their measurement protocol. Lastly, their study focused exclusively on Chinese patients with ankylosing spondylitis, and there is the possibility that SI joint deformities influenced the measurements.

The SI joint is as a potential source of lower back pain (6). However, for a joint which may be the source of low back pain in 15 – 25% of patients, there is limited literature on the anatomy of the SI joint (17). The importance of furthering our understanding of this joint is obvious when one recalls that low back pain is responsible for the loss of 17 million work days per year in the United States and accounts for about \$60 billion of the annual U.S. health care budget (18). The purpose of this paper was to provide more precise information on the dimensions and orientation of the SI joint using a new technique to radiographically evaluate the SI joint. Such information may be useful in surgical planning, in finding landmarks to assist in the surgical approach, and in performing SI joint injections (19).

Using the data described, surgeons and percutaneous-treatment specialists can better triangulate the location of the SI joint to help in treatment of SI joint pathology. We see other applications for this information and radiologic technique in the pelvic trauma, spine, and pain management arenas.

One potential limitation of this study was that the CT scans were performed with the patients lying supine, while most SI joint procedures are performed with a patient prone. It is doubtful that the bony anatomical landmarks change appreciably in this largely immobile joint. Since the measurements were made

off the pelvic-side as opposed to the iliac wing-side of the joint, the values should not change depending on whether the patient is supine or prone. Similarly, the relative distances from the ASIS and PSIS to the superior and inferior edge of the SI joint will not change based on the position of the patient.

Another potential limitation of this study is that the patients used for the study had clinical indications of abdominal and pelvic pain (and not necessarily with specific SI joint pain). This raises the question of whether there could be fundamental differences between the geometric features of the SI joint in patients with back or SI joint pain versus patients who do not have SI joint symptoms. Such differences could lend insight into the etiology of the disease or how manipulation of the SI joint toward the more normal condition could alleviate pain. At the present time, there are no studies or data to support the idea that such an anatomic difference exists between the normal and lower back pain-associated SI joint. Furthermore, it is doubtful that macroscopic changes in SI joint anatomy, as detectable by CT scanning, would be present in painful versus non-painful clinical conditions. In either case, this large scale study is the first to provide a detailed 3-D description of the SI joint in vivo among patients with pain. Future anatomical studies may serve to refine our views.

CONCLUSION

In summary, there is limited published, original literature describing detailed measurements of the SI joint. This is one of the first papers to provide relevant information of the location of the SI joints relative to easily palpable anatomic landmarks: the ASIS and PSIS. This information should help physicians localize the SI joint for percutaneous procedures, and aid surgeons in their surgical planning and approach to the SI joint. The ability to reformat the data from a regular CT scan in order to analyze and reconfigure the SI joint in multiple planes may also prove useful in serially evaluating the joint post-operatively, such as after a fusion. The use of this radiographic technique may also prove useful in studying the osteology of other bones, and circumventing the need to obtain these measurements from cadaveric specimens.

ACKNOWLEDGEMENTS

We thank Dr. Brandon Macias for his assistance with the statistical analysis.

REFERENCES

1. Bernard TN Jr, Kirkaldy-Willis WH. Recognizing specific characteristics of non-specific low back pain. *Clin Orthop Relat Res* 1987; 217:266-280.
2. Schwarzer A, Aprill C, Bogduk N. The sacroiliac joint in chronic low back pain. *Spine (Phila Pa 1976)* 1995; 20:31-37.
3. Bogduk N. International Spinal Injection Society guidelines for the performance of spinal injection procedures. Part 1: Zygapophysial joint blocks. *Clin J Pain* 1997; 13:285-302.
4. Maigne J, Aivaliklis A, Pfefer F. Results of sacroiliac joint double block and value of sacroiliac pain provocation tests in 54 patients with low back pain. *Spine (Phila Pa 1976)* 1996; 21:1889-1892.
5. Frymoyer J. *The Adult Spine: Principles and Practice*. 2nd ed. Lippincott-Raven, Philadelphia, 1997.
6. Cohen S. Sacroiliac joint pain: A comprehensive review of anatomy, diagnosis, and treatment. *Anesth Analg* 2005; 101:1440-1453.
7. Dreyfuss P, Dreyer S, Cole A, Mayo K. Sacroiliac joint pain. *J Am Acad Orthop Surg* 2004; 12:255-265.
8. Bowen V, Cassidy J. Macroscopic and microscopic anatomy of the sacroiliac joint from embryonic life until the eighth decade. *Spine (Phila Pa 1976)* 1981; 6:620-628.
9. Leshner J, Dreyfuss P, Hager N, Kaplan M, Furman M. Hip joint pain referral patterns: A descriptive study. *Pain Med* 2008; 9:22-25.
10. Elgafy H, Semaan H, Ebraheim N, Coombs R. Computed tomography findings in patients with sacroiliac pain. *Clin Orthop Relat Res* 2001; 382:112-118.
11. Maigne J, Boulahdour H, Chatellier G. Value of quantitative radionuclide bone scanning in the diagnosis of sacroiliac joint syndrome in 32 patients with low back pain. *Eur Spine J* 1998; 7:328-331.
12. Slipman C, Sterenfeld E, Chou L, Herzog R, Vresilovic E. The value of radionuclide imaging in the diagnosis of sacroiliac joint syndrome. *Spine (Phila Pa 1976)* 1996; 21:2251-2254.
13. Manchikanti L, Abdi S, Atluri S, Benjamin RM, Boswell MV, Buenaventura RM, Bryce DA, Burks PA, Caraway DL, Calodney AK, Cash KA, Christo PJ, Cohen SP, Colson J, Conn A, Cordner H, Coubarous S, Datta S, Deer TR, Diwan S, Falco FJ, Fellows B, Geffert S, Grider JS, Gupta S, Hameed H, Hameed M, Hansen H, Helm S 2nd, Janata JW, Justiz R, Kaye AD, Lee M, Manchikanti KN, McManus CD, Onyewu O, Parr AT, Patel VB, Racz GB, Sehgal N, Sharma ML, Simopoulos TT, Singh V, Smith HS, Snook LT, Swicegood JR, Vallejo R, Ward SP, Wargo BW, Zhu J, Hirsch JA. An update of comprehensive evidence-based guidelines for interventional techniques in chronic spinal pain. Part II: Guidance and recommendations. *Pain Physician* 2013; 16:S49-S283.
14. Wallace, M. Implantable Therapies for Spine Pain. UC San Diego Orthopaedic Spine Surgery Conference, February 6, 2009.
15. Zou YC, Li YK, Yu CF, Yang XW, Chen RQ. A cadaveric study on sacroiliac joint injection. *Int Surg* 2015; 100:320-327.
16. Rupert M, Lee M, Manchikanti L, Datta S, Cohen S. Evaluation of sacroiliac joint interventions: A systematic appraisal of the literature. *Pain Physician* 2009; 12:399-418.
17. DePalma M, Ketchum J, Saullo T. What is the source of chronic low back pain and does age play a role? *Pain Medicine* 2011; 12:224-233.
18. McCulloch J, Transfeldt E. Epidemiology and natural history of spondylogenic backache. In: *Macnab's Backache*. Macnab's Backache by J. A. McCulloch and E. E. Transfeldt, 795 pages. Published 1997. 3rd Edition Williams & Wilkins, Baltimore, MD. pp 240-246.
19. Fortin J, Sehgal N. Sacroiliac joint injection and arthrography with imaging correlation. In: Lennard T (ed). *Pain Procedures in Clinical Practice*. Hanley & Bel-fus, Inc, Philadelphia, 2000, pp 265-275.